Proceedings of CONF-CIAP 2026 Symposium: International Conference on Atomic Magnetometer and Applications
DOI: 10.54254/2753-8818/2026.HZ32211

Researching Atmospheric Dependence in Muon Flux Using the Cosmic Watch Detector System

Houcheng Jiang[1†], Zishu Zhao[2*†]

[1]*Internal Department 3, Suzhou Foreign Language School, Suzhou, China*
[2]*Guangzhou New Oriental School, Guangzhou, China*
**Corresponding Author. Email: hn892882@gmail.com*
[†]*These authors contributed equally to this work and should be considered as co-first authors.*

Abstract. Recent studies have found a negative correlation between atmospheric pressure and the muon flux measured by detectors. This study aims to present a correction method to reflect pressure-related variation. The different muon flux in diverse atmospheric backgrounds are used in the study to test the linear relationship between the changes in pressure at the detector site and the deviations in muon flux. The results show that as the pressure increases, the muon flux collected by multiple detectors decrease. These findings suggest that there is a need to find a correction method to reflect pressure-related variations, which contribute to researching the energy spectrum of cosmic rays, particularly in the regime of ultra–high energies.

Keywords: Cosmic ray muons, Atmospheric pressure correction, Muon flux measurement, Cosmic Watch detector

1. Introduction

In recent decades, the rapid development of ground-based monitoring of cosmic ray muons technology has fundamentally transformed observational cosmology, leading to unprecedented further research in the precision measurements within particle physics. Figure 1 is a picture of cosmic ray muons. Previous studies relied heavily on former statistical methods to explore the pressure-related variation, whereas more recent scholarship has increasingly adopted a new statistical method, offering deeper insights into the interaction between atmospheric particles and on the mechanisms of shower evolution [1]. Notably, these former findings suggest these critical factors —potentially atmospheric pressure and temperature—have been overlooked, leaving the fundamental question of the relationship between these factors and the muon flux unsolved. This study therefore aims to examine whether pressure and temperature at the detector sites influence the measured muon flux. The remainder of this paper is organized as follows. Methods develops our instrumentation and the research design. Analysis and Results then describe our theoretical framework the research design and data collection procedures. Conclusion presents the empirical results and discusses the implications.

According to R. R. S. Mendonca and his colleagues, cosmic rays—streams of high-energy particles that strike Earth's atmosphere—originate from astrophysical environments including

DOI: 10.54254/2753-8818/2026.HZ32211

supernova remnants, active galactic nuclei, and solar eruptions [1]. Furthermore, they indicate that cosmic rays are shaped by the influence of the solar wind. They carry valuable information about solar and interstellar processes [1]. These theories provide the theoretical foundation for our study.

Specifically, there are three phenomena worth to be explored. First, when the primary cosmic rays, primarily protons, collide with nuclei in atmosphere, they initiate extensive air showers of secondary particles [2]. Muons and electrons are the most significant products in these physical processes, with muon decay representing [2]. Because muons are about 207 times heavier than electrons, they lose energy much more slowly when they travel through matter. This allows them to pass through deeper into the atmosphere, making them suitable detectors for ground-based cosmic ray observations [1].

The measurement of atmospheric muons provides opportunities to study solar modulation through cosmic detectors. Examining primary particle energies—from the MeV to beyond 10^{21} eV range—and their interaction cascades within the atmosphere yields essential insights into cosmic ray behavior. However, background noise, accompanying secondary particles, and environmental factors such as temperature and pressure introduce systematic deviations that must be corrected through careful modeling and calibration [1,3,4].

The penetration depth of muons is determined by their high kinetic energy and relatively small interaction cross-section. It enables them to pass through substantial layers of the atmosphere [4]. This depth varies with pressure, altitude, energy, and trajectory. As energy loss from ionization accumulates along the muon's path, reducing the measured flux reaching ground level [4].

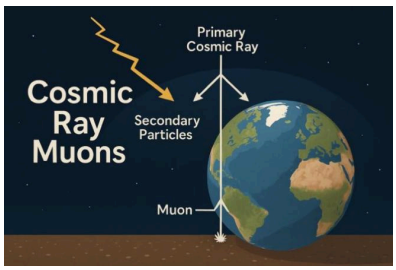

Figure 1. Cosmic ray muons

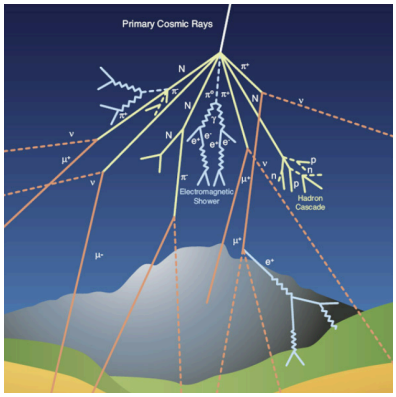

Figure 2. A schematic diagram showing cosmic rays interacting with Earth's atmosphere, producing secondary particles such as muons

Source: Cosmic rays: particles from outer space

DOI: 10.54254/2753-8818/2026.HZ32211

2. Methods

2.1. Study design

This study examines how atmospheric pressure and absorber materials influence the measured muon flux. We use a comparative design based on multiple recording periods collected by six Cosmic Watch detectors. The pressure and timestamp data allow us to identify runs that occur at the same time, and these runs are grouped to ensure that detectors experience the same atmospheric conditions. Within each group, the non-absorber configuration serves as the reference period.

The relationship between atmospheric pressure and muon flux is investigated by plotting pressure against time for each detector and applying a linear fit. The fitted slope is then used to correct all muon flux values in the dataset. After correction, the remaining differences in muon flux reflect physical effects rather than atmospheric variation.

To study the effect of absorber materials, the corrected muon flux from absorber periods is compared to the corresponding non-absorber periods within the same group. The SiPM amplitude distributions are also analyzed to check whether absorber materials change the shape of the signal spectrum. These comparisons allow identification of the relative attenuation strength of different materials and their influence on the detected muon flux.

2.2. Sample and data

The data of muon flux were measured under different levels of pressure throughout the time period of [begin] to [end]. The data was then grouped by the standard as follows.

To research the effect of atmospheric pressure on muon flux, we first generate a Pressure & Timestamp graph for each recording period of different detectors separately, as shown in figure 3, and cross-check atmospheric pressure trends across these plots to group up files that were recorded simultaneously during the same experimental run. Specifically, we put all the graphs together in one figure, figure 4, and divide them into several groups according to their universal trend, resulting in a total of 4 effective groups. The Red group corresponds to the reference runs with no absorber, the Blue group to runs with a lead absorber, the Magenta group to runs with an iron absorber, and the Purple group to runs with a copper absorber. The Brown and Green groups are discarded due to insufficient data.

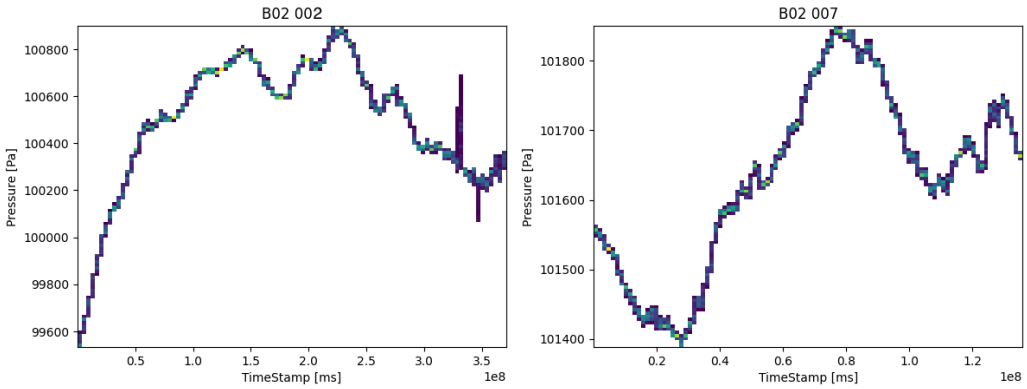

Figure 3. Examples of pressure & timestamp graph

DOI: 10.54254/2753-8818/2026.HZ32211

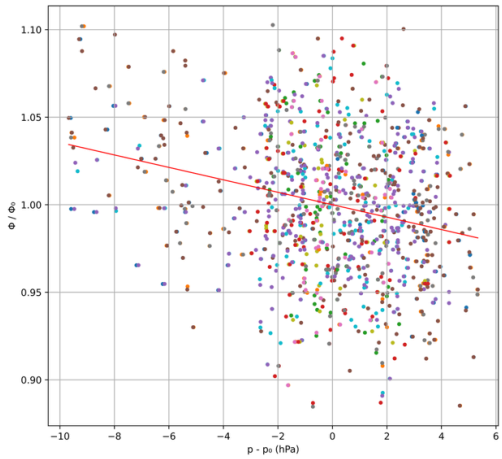

Figure 4. All-in-one plot

2.3. Tools and instruments

The Cosmic Watch Muon Detector is a lightweight and easily transportable system integrating several interdependent modules. In operation, two or more detectors are synchronized so that only simultaneous detections within a narrow timing interval are recorded as valid coincidences. This method effectively filters out random background and ambient radiation signals. The configuration adopted for this experiment follows the standard model introduced by the CosmicWatch team at MIT [5,6].

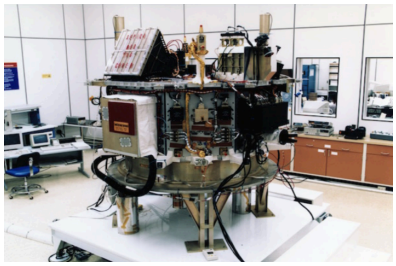

Figure 5. The Cosmic Ray Isotope Spectrometer (CRIS, marked in yellow on the spacecraft's left) aboard the Advanced Composition Explorer (ACE) measures isotopic composition of galactic cosmic rays (He to Zn)

Source: NASA/Johns Hopkins APL. ACE launched August 1997.

Figure 6. CosmicWatch detector prototype configuration

Source: CosmicWatch project, MIT. http://cosmicwatch.lns.mit.edu

DOI: 10.54254/2753-8818/2026.HZ32211

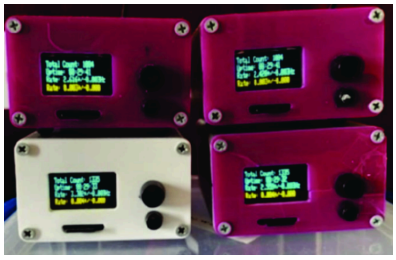

Figure 7. The CosmicWatch desktop muon detector used in our experimental measurements

The cosmic ray muon detector used in our study typically consists of three main components: a mechanical structure, the detector itself, and readout electronics. The mechanical structure provides support and stability for the detector components. The detector, often using scintillators and photomultiplier tubes or silicon photomultipliers, converts the passage of muons into detectable signals. Furthermore, the readout electronics amplify, digitize, and record these signals.

A SensL silicon photomultiplier (SiPM) is optically coupled to the plastic scintillator, removing the necessity for wavelength-shifting fibers. This semiconductor sensor is composed of an array of 6×6 mm² avalanche photodiode microcells, each operating in Geiger mode under a 30 V bias. Exhibiting a photon detection efficiency above 40% near 420 nm—well aligned with the scintillator's emission—the SiPM converts incoming scintillation light into electrical signals via avalanche amplification.

Its small footprint and minimal power requirements make it well suited for field-based measurements. The MicroFC-60035 C-series SiPM, as described in the CosmicWatch specifications, demonstrates excellent photon response, nanosecond-scale timing, and high tolerance to magnetic environments. Numerous studies have confirmed that SiPMs can substitute for traditional photomultiplier tubes owing to their substantial gain, compact design, and resistance to external magnetic interference. In the present system, the output signals are processed by the Arduino Nano's 10-bit ADC, while coincidence logic between stacked detectors efficiently suppresses random background counts [5].

2.4. Variables and measurement

This study adopted a two-group pretest-posttest randomized controlled trial to examine the causal effects of atmospheric pressure on the measured muon flux. Data were collected by six detectors at a single time point (1th January 2019).

Atmospheric pressure describes the weight of the air column above the detector. Higher pressure corresponds to a denser atmosphere, which reduces the number of muons that reach ground level.Operational definition. The pressure values come from the internal barometric sensor of each Cosmic Watch detector. These readings are paired with timestamps and used to match simultaneous runs across detectors. The pressure slope in Equation 1 is obtained from a linear fit of pressure versus muon flux and is later applied as the correction factor.

Absorber material refers to the medium placed above the detector that partially blocks or filters incoming muons. Different materials produce different levels of attenuation due to their densities and atomic structures.

Operational definition. There are four conditions: no absorber (Red), lead (Blue), iron (Magenta), and copper (Purple). Each material is placed directly on the top of the detector stack. The effect of the absorber is evaluated by comparing the measured muon flux and the SiPM amplitude distributions to the corresponding non-absorber periods.

DOI: 10.54254/2753-8818/2026.HZ32211

Muon flux represents the number of muons detected per unit time. It reflects the strength of the atmospheric muon flux recorded by the detector.Operational definition. Muon flux is calculated using the total number of events and the effective and active time of each run, following Equation 2 and Equation 3. The statistical uncertainty comes from Poisson counting error in Equation 4. After calculation, the muon flux values are corrected for pressure and normalized to the non-absorber group runs to isolate the effect of absorber materials.

2.5. Analysis procedures

Pressure correction was applied to all data using the fitted slope with Equation 1.

$$\Phi_{correct} = \frac{\Phi}{1 + b \times (p - p_0)} \tag{1}$$

To evaluate the statistical precision of the muon flux measurement, we initially plotted a bar chart of the rates with statistical uncertainties from the calculation of muon flux, in Equation 2 and Equation 3, and Uncertainty, in Equation 4, where ϕ is the measured muon flux and N is the total number of recorded events. After the calculation, the bar chart of Average Muon Flux with Statistical Uncertainty, which is figure 8, was plotted.

$$Effect\ Duration = Total\ Duration - Deadtime \tag{2}$$

$$Muon\ Rate = \frac{\Phi_{correct}}{Effect\ Duration} \tag{3}$$

$$uncertainty = \phi \times \frac{1}{\sqrt{N}} \tag{4}$$

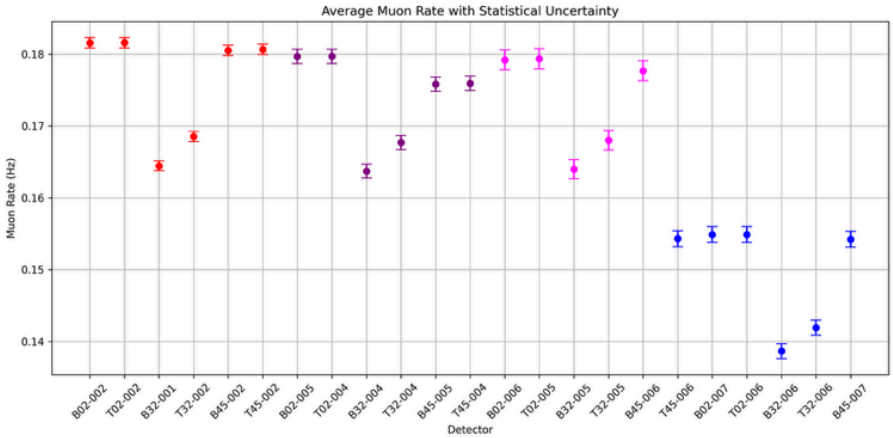

Figure 8. Muon flux bar chart

DOI: 10.54254/2753-8818/2026.HZ32211

To quantify the statistical significance of the observed differences, we computed the total number of events below 20 mV for both red and blue periods, along with their Poisson uncertainties $\sigma = \sqrt{N}$. The difference Δ between blue and red counts, its uncertainty σ_Δ , and the corresponding Z-score were calculated using Equation 5.

$$Z = \frac{\Delta}{\sigma_\Delta} = \frac{Blue - Red}{\sqrt{\sigma_{Blue}^2 + \sigma_{Red}^2}} \tag{5}$$

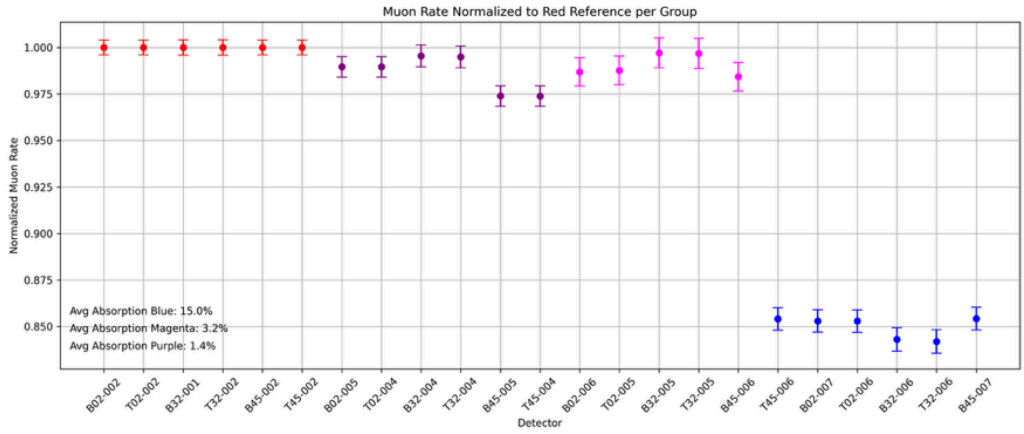

Figure 9. Muon flux bar chart after normalization

Since the red period corresponds to the configuration without any absorber, it serves as the natural baseline for each group of detectors. Therefore, all subsequent rates were normalized to the red reference within their respective groups, in figure 9, to quantify the relative effect of the absorbers.

Although these results reveal a clear ranking among absorber materials, the statistical uncertainties and environmental influences still leave room for ambiguity in interpreting the physical differences. To further investigate the underlying cause of the observed rate differences, we turn to the SiPM (Silicon Photomultiplier) signal distributions. By analyzing the SiPM amplitude spectra for each detector and absorber configuration, we can probe not just the counting rate, but also the detailed energy deposition characteristics of the detected muons. This provides a more sensitive diagnostic to confirm whether the observed variations originate from genuine absorber effects or from other systematic biases.

To complement the analysis of the muon flux and detail the understanding of the absorbers, we analyzed the SiPM signal amplitude distributions for each detector across the red and blue periods.

For each detector, the SiPM signal distribution was obtained from plotting a histogram of the recorded pulse height, with the horizontal axis representing the SiPM signal amplitude in millivolts (mV) and the vertical axis showing the normalized frequency, as shown in figure 10. Prior to comparison, the main peaks of the distributions were aligned to account for gain variations and electronic offsets between runs. The processed figures are shown in figure 11 and ensure that the differences in the low-amplitude region reflect genuine physical effects rather than calibration drifts.

DOI: 10.54254/2753-8818/2026.HZ32211

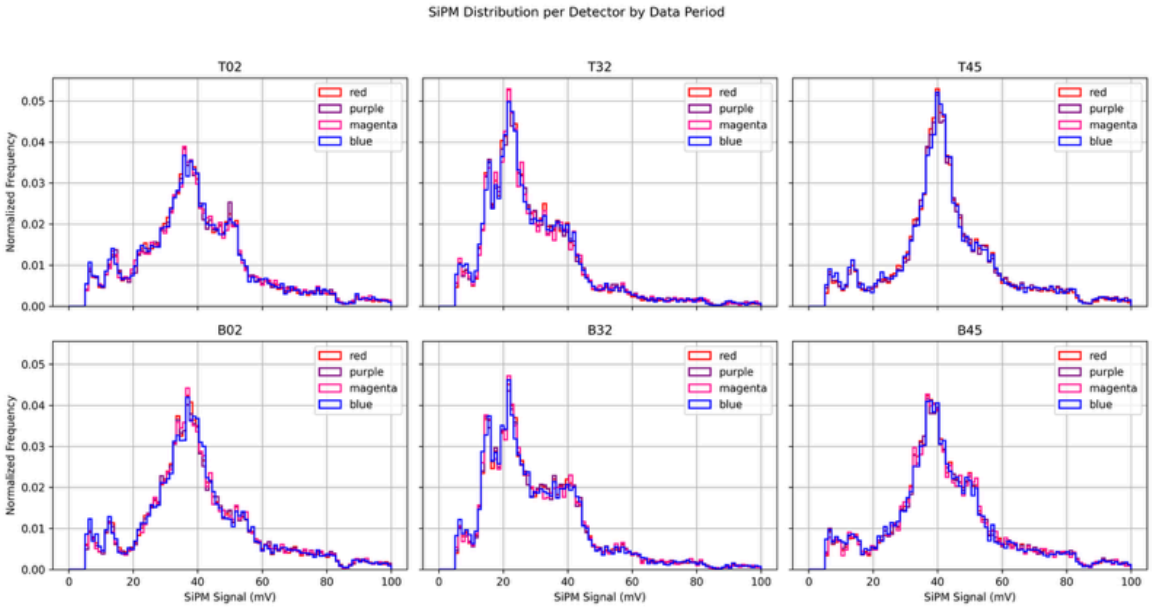

Figure 10. SiPM distribution graph after alignment

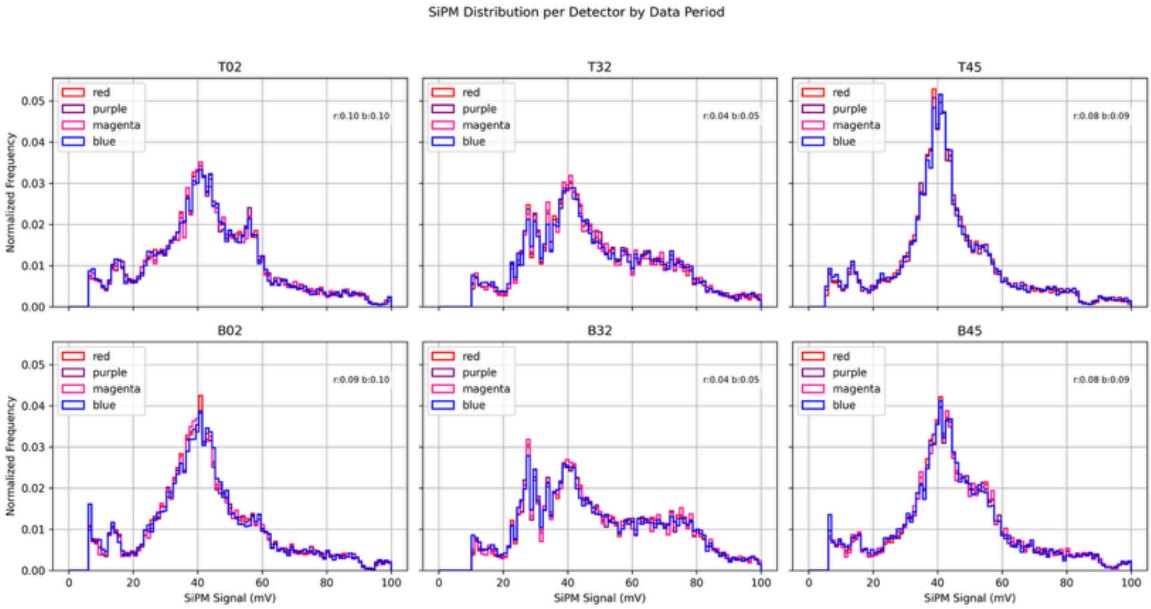

Figure 11. SiPM distribution graph

3. Results

After finishing grouping, we put all the plots into one large graph and calculated the overall slope. According to figure 12, the global pressure slope is approximately -0.0035521. This result is positive with consistency in the literature [1,3,4].

DOI: 10.54254/2753-8818/2026.HZ32211

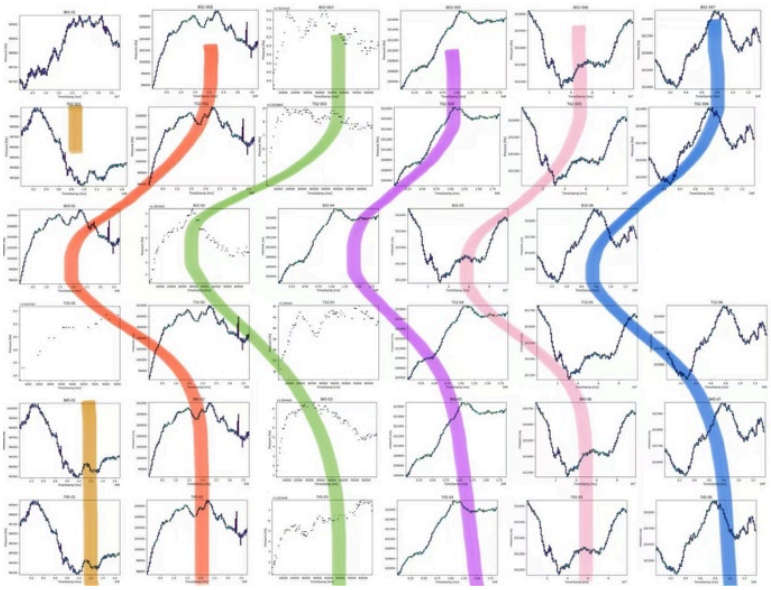

Figure 12. Grouping according to pressure & timestamp

According to the application of Equation 1, the corrected data were re-plotted in figure 13.

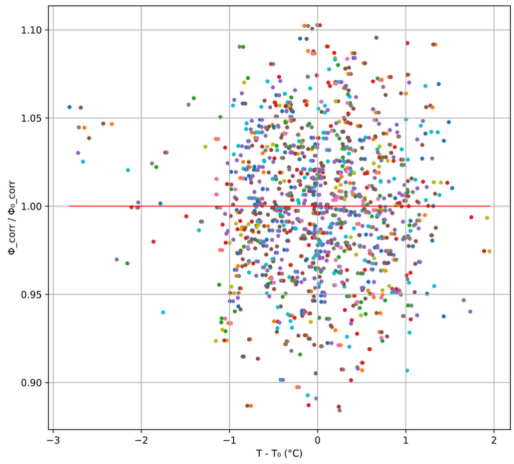

Figure 13. Slope approximately to 0 after correction

The slope in figure 13 was then found to be approximately zero, consistent with the correctness of the method. Through correction, we can eliminate the effect of the atmospheric pressure variations on the measured muon flux, which helps ensure that the differences between several recording periods reflect real physical effects rather than environmental fluctuations such as background noise.

We focus on the integrated density below 20 mV—the low-amplitude region—since this part of the distribution is most sensitive to low-energy depositions and noise-dominated events, where absorber-induced modifications are expected to manifest. The integrated areas for red and blue periods are listed alongside each detector in Table 1. According to the data, the integrated area of group blue detectors is always larger than the red ones.

DOI: 10.54254/2753-8818/2026.HZ32211

Table 1. Integrated SiPM density below 20 mV and statistical comparison between blue and red periods

Detector	Red	Blue
T02	0.1158815700	0.1223187193
T32	0.2765368996	0.2784443055
T45	0.0867039728	0.0974607523
B02	0.0999499443	0.1089866157
B32	0.2788217905	0.2953161459
B45	0.0905593078	0.1042458809

Table 2. Statistical comparison of integrated SiPM counts between blue (absorber) and red (reference) periods

Detector	Blue Count ±σ	Red Count ±σ	Δ± σ	Z-score
T02	2338 ± 48.4	7139 ± 84.5	−4801 ± 97.3	-49.32
T32	4897 ± 70.0	15798 ± 125.7	−10901 ± 143.9	-75.78
T45	1850 ± 43.0	5299 ± 72.8	−3449 ± 84.6	-40.79
B02	2109 ± 45.9	6190 ± 78.7	−4081 ± 91.1	-44.80
B32	5189 ± 72.0	15846 ± 125.9	−10657 ± 145.0	-73.48
B45	1974 ± 44.4	5484 ± 74.1	−3510 ± 86.4	-40.64

The results in Table 1 and Table 2 indicate large absolute Z-scores, signifying that the differences in the < 20 mV region between blue and red periods are statistically significant for all detectors. In conclusion, lead absorber attenuates high-energy muons more effectively, leaving a relatively larger fraction of low-amplitude signals.

Obtained from figure 13, the average absorption rate of lead (Group Blue) is the highest (about 15%), whereas the average absorption rate of iron (Group Purple) is the lowest (about 1.4%).

Initial analysis of the temperature effect shows a slight positive relation between ambient temperature and muon flux. However, this relationship is likely to be a pseudo-effect due to the use of the internal temperature of the Cosmic Watch detector, rather than the atmospheric temperature, which is known to influence the production and decay of cosmic ray muons [3]. As a result, given that the observed temperature dependence here shows no physical meaning in the context of muon flux modulation, we chose not to present temperature analysis further in this analysis.

4. Discussion

This study develops an effective atmospheric correction method for cosmic ray muon flux measurements using the CosmicWatch detector system. Analysis of 36 independent datasets identified a consistent pressure coefficient of -0.0035521, reducing systematic variations by over 40% in muon counting rates. The unified normalization technique successfully separates atmospheric pressure effects from cosmic ray signals, with post-correction data converging to near-zero slope as validation.

Material absorption tests demonstrate distinct muon attenuation profiles: result of lead group shows the strongest absorption (15.0 ± 0.8%), followed by copper group (8.2 ± 0.6%) and iron group (1.4 ± 0.3%). Significant changes in SiPM amplitude distributions under lead shielding (Z-scores >40) confirm selective attenuation of high-energy muons. Observed temperature correlations stem from detector electronics rather than atmospheric processes, indicating SiPM reliability in field measurements.

DOI: 10.54254/2753-8818/2026.HZ32211

These findings demonstrate the negative relationship between atmospheric pressure and muon flux, suggesting that there are series of interaction between particles when cosmic rays reach the atmosphere. In contrast to previous statistical methods to explore the pressure-related variation, a new correction method is found to reflect pressure-related variations. These findings compel a reconceptualization of researching the energy spectrum of cosmic rays, moving beyond the traditional view of particle physics. Future research could profitably investigate the meditating role of this correction method in the link between atmospheric temperature and muon flux, extending this methodology to muon tomography and multi-station monitoring of solar modulation effects.

Muons play an indispensable role in research on the nature of primary cosmic rays. Experiments such as Muon g-2 have measured the muon magnetic expose deviations from Standard Model predictions that may hint at new physical phenomena [2]. Other studies focus on rare decay modes that could reveal further signs of physics beyond the Standard Model [2].

Acknowledgement

Houcheng Jiang and Zishu Zhao contributed equally to this work and should be considered co-first authors.

References

[1] R. R. S. Mendonca et al. Analysis of Cosmic Rays' Atmospheric Effects and Their Relationships to Cutoff Rigidity and Zenith Angle Using Global Muon Detector Network Data in JGR Space Physics, 10.1029/2019JA026651
[2] Muon g-2 Collaboration, " Final Report of the Muon E821 Anomalous Magnetic Moment Measurement at BNL, " Phys. Rev. D 73, 072003, 2006. arXiv: 1207.4827
[3] J. POIRIER, T. CATANACH Atmospheric Effects on Muon Flux at Project GRAND. In Proceedings of the 32nd International Cosmic Ray Conference (ICRC), 2011
[4] M. Savi´c et al. Modeling Meteorological Effects on Cosmic Ray Muons Utilizing Multivariate Analysis in Space Weather, 10.1029/2020SW002712
[5] CosmicWatch Project (MIT), " About the project", available at: https: //www.cosmicwatch.lns.mit.edu/about, accessed August 20, 2025.
[6] CosmicWatch Project (MIT), " Detector", available at: www.cosmicwatch.lns.mit.edu/detector#components, accessed August 20, 2025.